Proton structure and hard p-p processes at LHC energies

Gennady Lykasov

JINR, Dubna,

CONTENT

1. Intrinsic quark-antiquark pair distribution in proton.
2. Some attempts to search for these states from different inclusive processes.
3. Advantage of semi-inclusive processes $pp \rightarrow \gamma/Z/W$ + c-jet for this searching.
4. Constraints on the intrinsic charm (**IC**) content of proton from ATLAS data.
5. Other predictions for the **IC** contribution in $pp \rightarrow Z$ + c-jet process.
6. Non perturbative gluon distribution in proton.
7. Application of these distributions in soft and hard p-p processes at LHC energies.
8. Dielectron emission in hadron reactions and the electromagnetic form factor at the time-like kinematical region.

I. Intrinsic Q-Q states in proton and their searching.

BHPS model: S.J. Brodsky,P. Hoyer, C. Peterson and N.Sakai, Phys.Lett.B9(1980) 451; S.J. Brodsky, S.J. Peterson and N. Sakai, Phys.Rev. D23 (1981) 2745.

Intrinsic $Q\bar{Q}$ in proton

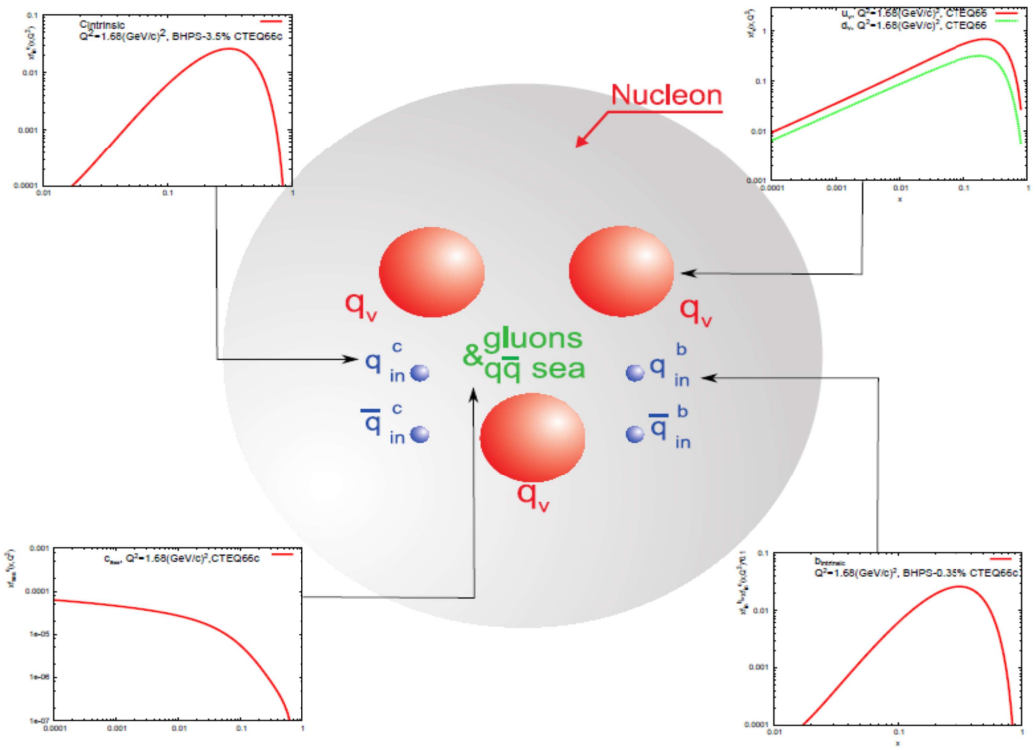

CHARM QUARK DISTRIBUTIONS IN PROTON

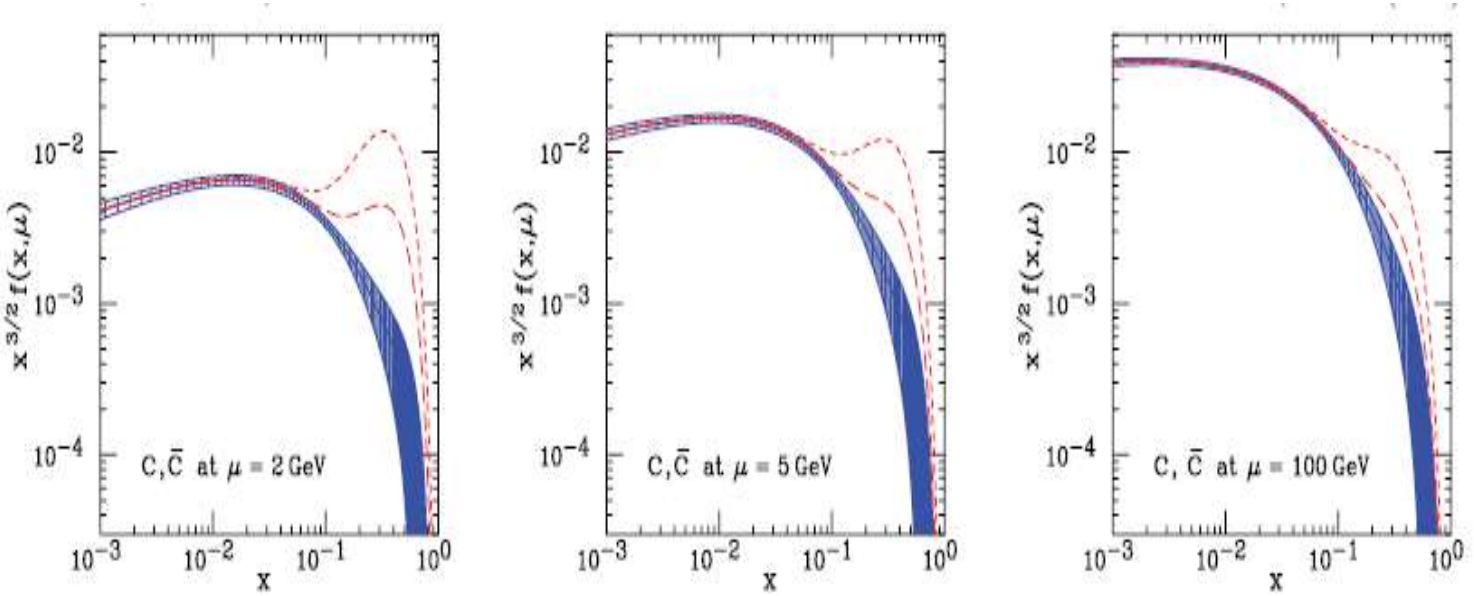

Charm quark distributions within the BHPS model. The three panels correspond to the renormalization scales $\mu = 2, 5, 100$ GeV respectively. The long-dashed and the short-dashed curves correspond to $\langle x_{c\bar{c}} \rangle = 0.57\%, 2.\%$ respectively using the PDF CTEQ66c. The solid curve and shaded region show the central value and uncertainty from CTEQ6.5, which contains no ***IC***.

There is an enhancement at x>0.1 due to the IC contribution

Some attempts to search for the intrinsic charm (IC) in proton

1. Forward production of hadrons consisting of non charmed and charmed quarks (Λ_c, Σ_c ,etc., or D-mesons) at ISR energies.

Difficulties: a big sensitivity of inclusive spectra to the fragmentation functions (up to 50 % and more) of quarks to c-hadrons and large experimental statistics and systematics uncertainties (up to 100% and even more) .

2. EMC experiment -measurements of proton and nuclear structure functions in DIS at large momentum fractions x.

Difficulties: very big experimental error bars at large x and large QCD scale uncertainties.

3. ICE cube experiment: a measurement of the neutrino flux in an ice cube produced from decay of charmed hadrons created in cosmic rays.

Difficulties: huge experimental error bars (about few orders) at neutrino energies about 10^6 GeV, where the IC signal was predicted.

4. Inclusive production of D-mesons at LHCb.

Difficulties: unreachable p_T region where the IC signal was predicted.

PHOTON (DI-LEPTON) AND c(b)-JETS PRODUCTION IN P-P

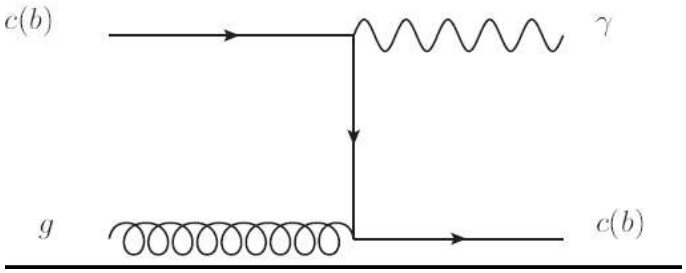

Fig.a. Feynman diagram for the process $c(b)+g\rightarrow\gamma+c(b)$

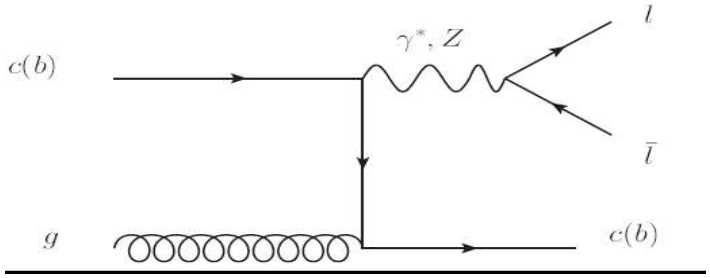

Fig.b. Feynman graph for the process $c(b)+g\rightarrow\gamma/Z^0+c(b)$

$$x_F=\frac{2p_T}{s^{1/2}}sh(\eta);p_{T\gamma}=-p_{Tc}.$$

$$x_{c(b)}=\frac{m^2_{l^+l^-}}{x_g s}+x^f_{c(b)}$$

To observe the IC for Fig.a and Fig.b

$$x_c\geq x_F>0.1$$

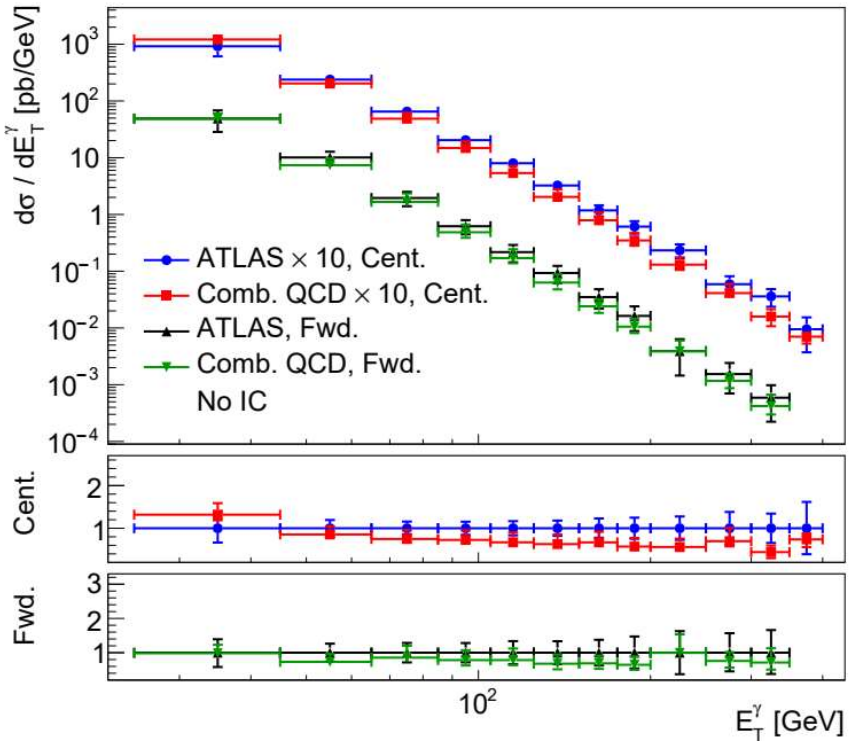

(a) $w_c = 0$ %

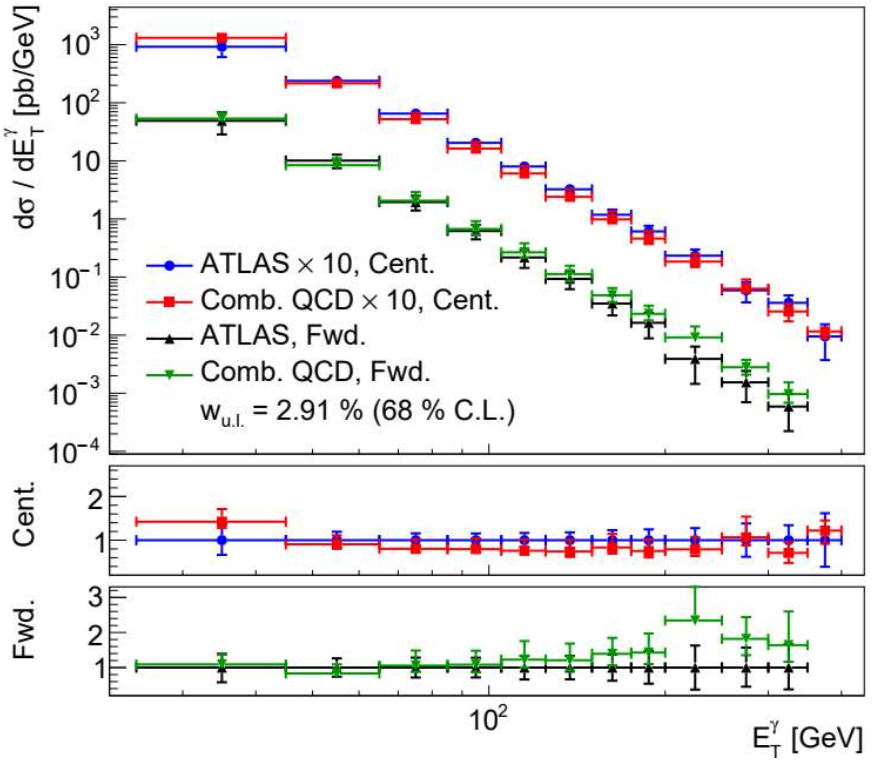

(b) $w_{u.l.} = 2.91$ %

The transverse energy spectrum of photons calculated within combined QCD compared with ATLAS data: at small x the k_T- factorization is used, at x>0. 1 the collinear QCD is used.

(a) top: the spectrum at central rapidity region $|\eta^\gamma| < 1.37$ and forward $1.56 < |\eta^\gamma| < 2.37$ region without the IC contribution;

(a) middle: the ratio of the MC calculation to the data for the central rapidity region ($w_c = 0\%$);

(a) bottom: the ratio of the MC calculation to the data for the forward rapidity region ($w_c = 0\%$)

(b): the same spectra, as in (a), but with the upper limit of IC contribution $w_{u.l.} = 2.91$ %.

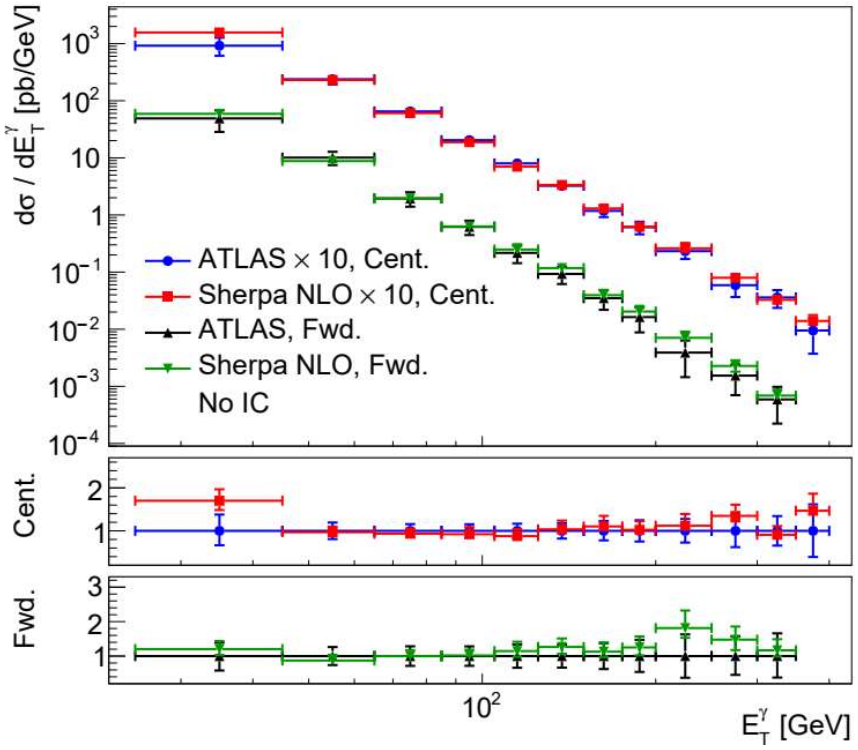

(a) $w_c = 0$ %

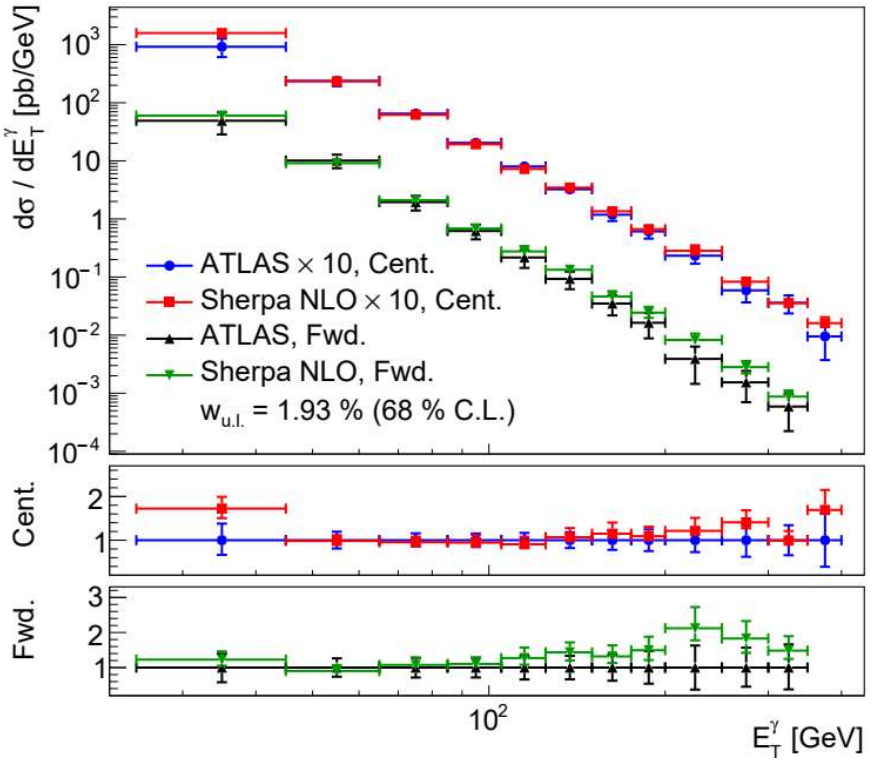

(b) $w_{u.l.} = 1.93$ %

The transverse energy spectrum of photons calculated within SHERPA (NLO) compared with ATLAS data.

(a) top: the spectrum at central rapidity region $|\eta^\gamma| < 1.37$ and forward $1.56 < |\eta^\gamma| < 2.37$ region without the IC contribution;

(a) middle: the ratio of the MC calculation to the data for the central rapidity region ($w_c = 0\%$);

(a) bottom: the ratio of the MC calculation to the data for the forward rapidity region ($w_c = 0\%$)

(b): the same spectra, as in (a), but with the upper limit of IC contribution $w_{u.l.} = 1.93$ %.

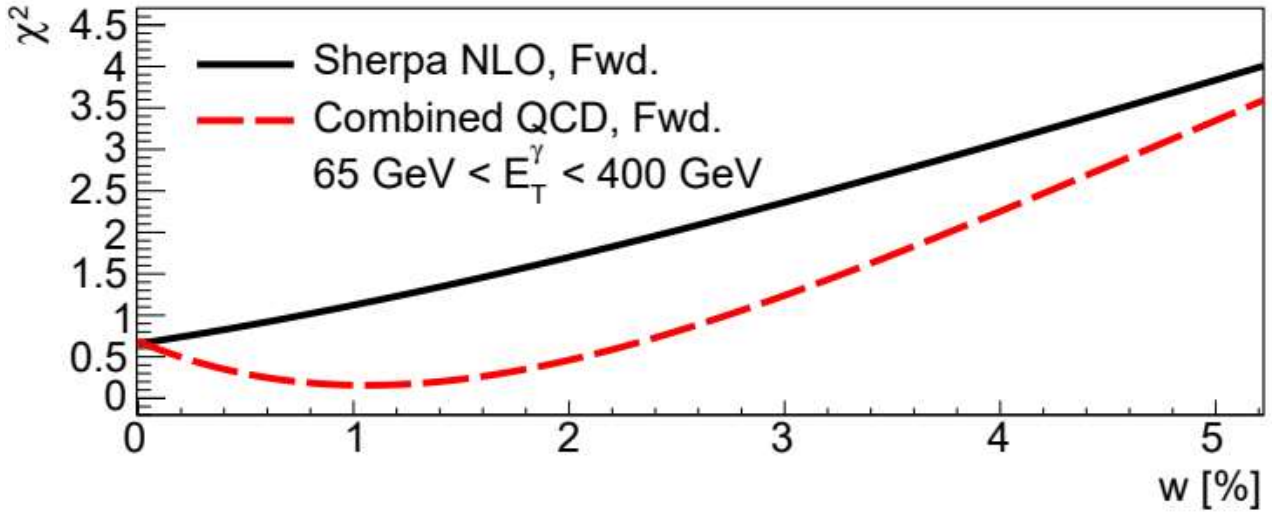

Solid line: $\chi 2$ as a function of w at the forward rapidity region in SHERPA NLO. is the same as the solid line but $\chi 2$ obtained within the combined QCD calculation.

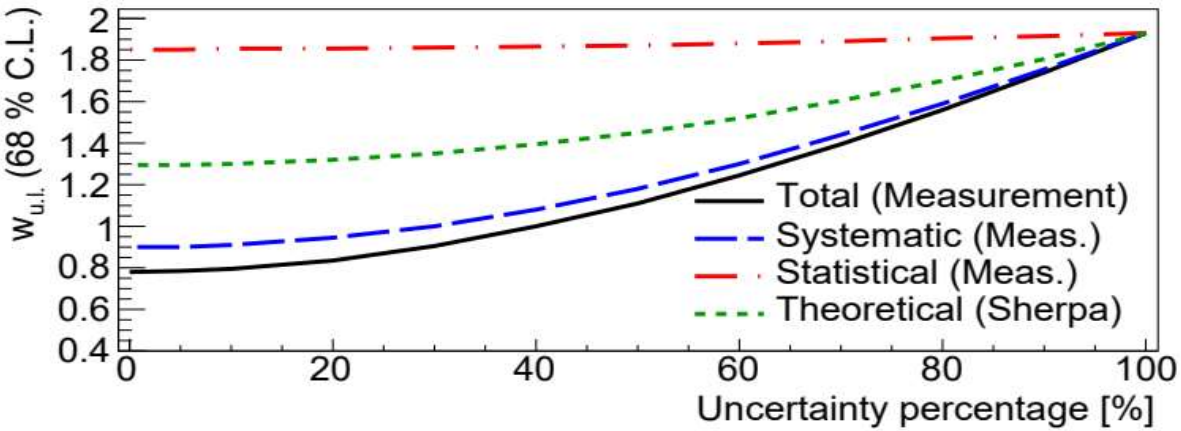

The dependence of the IC upper limit $w_{u.l.}$ at 68% C.L. on the uncertainty percentage of the particular uncertainty component.

ArXiv: 1712.09096 [hep-ph], August 2018, Eur.Phys.J C (in press)

What kind of observables is preferable to search for the IC at ATLAS ?

1. The single ratio σ (Z+c)/σ(Z+b)

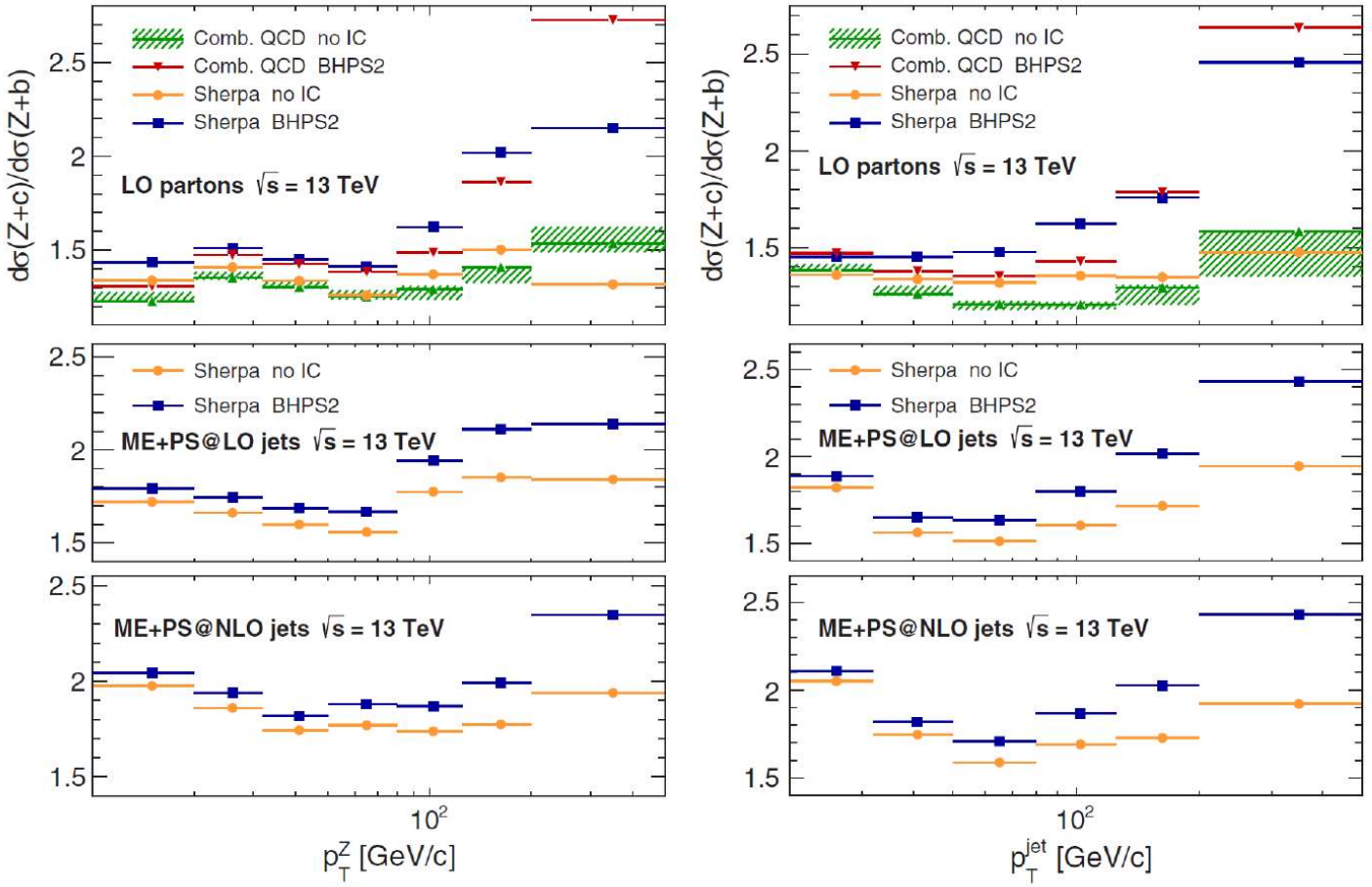

FIG. 6. Predictions for the ratio of the production cross sections of the $Z + c$ jet and of $Z + b$ jet as a function of the Z boson (left) and HF-jet (right) transverse momenta in the forward rapidity region $1.5 < |y^Z| < 2.5$ at $\sqrt{s} = 13$ TeV. The predictions are made with the SHERPA generator at the parton level using the LO matrix element (top panels) and at the particle level using the ME+PS@LO (middle panels) and ME+PS@NLO (bottom panels) models. Predictions of the combined QCD are also shown in the top panel. CTEQ66(C) PDF sets with no IC and BHPS2 fit are used.

A.V. Lipatov, G.L., M.A. Malyshev, A.A. Prokhorov, S.M. Turchikhin;
Phys.Rev. D97 (2018) no.11, 114019

2. The double ratio $(\sigma_f(Z+c)/\sigma_c(Z+c))/(\sigma_f(Z+b)/\sigma_c(Z+b))$

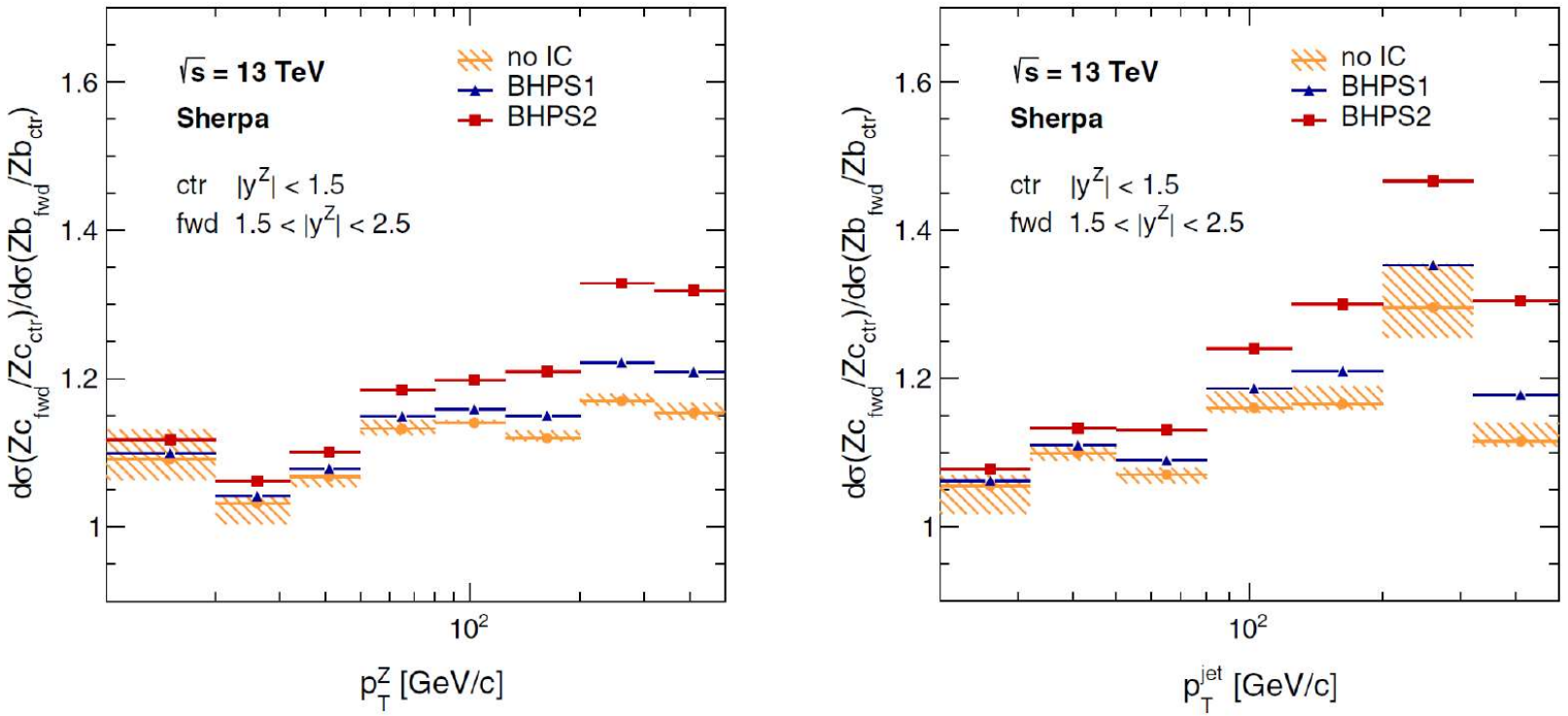

FIG. 7. Predictions for the double ratio as a function of the Z boson (left) and HF-jet (right) transverse momenta at $\sqrt{s} = 13$ TeV. The double ratio is the ratio of the $Z + c$-jet production cross section in the forward region $1.5 < |y^Z| < 2.5$ to the cross section in the central region $|y^Z| < 1.5$, divided by the same ratio for $Z + b$-jet production. The predictions are made with the SHERPA generator using the CT14NNLO PDF with different values of the IC contribution that correspond to BHPS1 and BHPS2 fits and without IC (no IC). The uncertainty bands represent the uncertainties in the QCD scale (shown only for no IC predictions).

A.V. Lipatov, G.L., M.A. Malyshev, A.A. Prokhorov, S.M. Turchikhin;

Phys.Rev. D97 (2018) no.11, 114019

II. Gluon distribution and hard p-p processes

SOFT PP -> h X

The inclusive spectrum is presented in the following form:

$$\rho(x=0,p_t)=\rho_q(x=0,p_t)+\rho_g(x=0,p_t)$$

Here $\rho_q = g\left(\frac{s}{s_0}\right)^{\Delta} \varphi_q;\ \varphi_q(0,p_t) = A_q \exp(-b_q p_t)$

$$\rho_g = g\left[\left(\frac{s}{s_0}\right)^{\Delta} - \sigma_{nd}\right]\varphi_g;\ \varphi_g(0,p_t) = \sqrt{p_t} A_g \exp(-b_g p_t)$$

$A_q = 11.91 \pm 0.39,\ b_q = 7.29 \pm 0.11$

$A_g = 3.76 \pm 0.13 \quad b_g = 3.51 \pm 0.02$

$g \approx 21$ mb

$\Delta \approx 0.12$

V.A. Bednyakov, A.V. Grinyuk, G.L., M. Poghosyan, Int. J.Mod.Phys. A 27 (2012) 1250012. hep-ph/11040532 (2011); hep-ph/1109.1469 (2011); Nucl.Phys. B 219 (2011) 225.

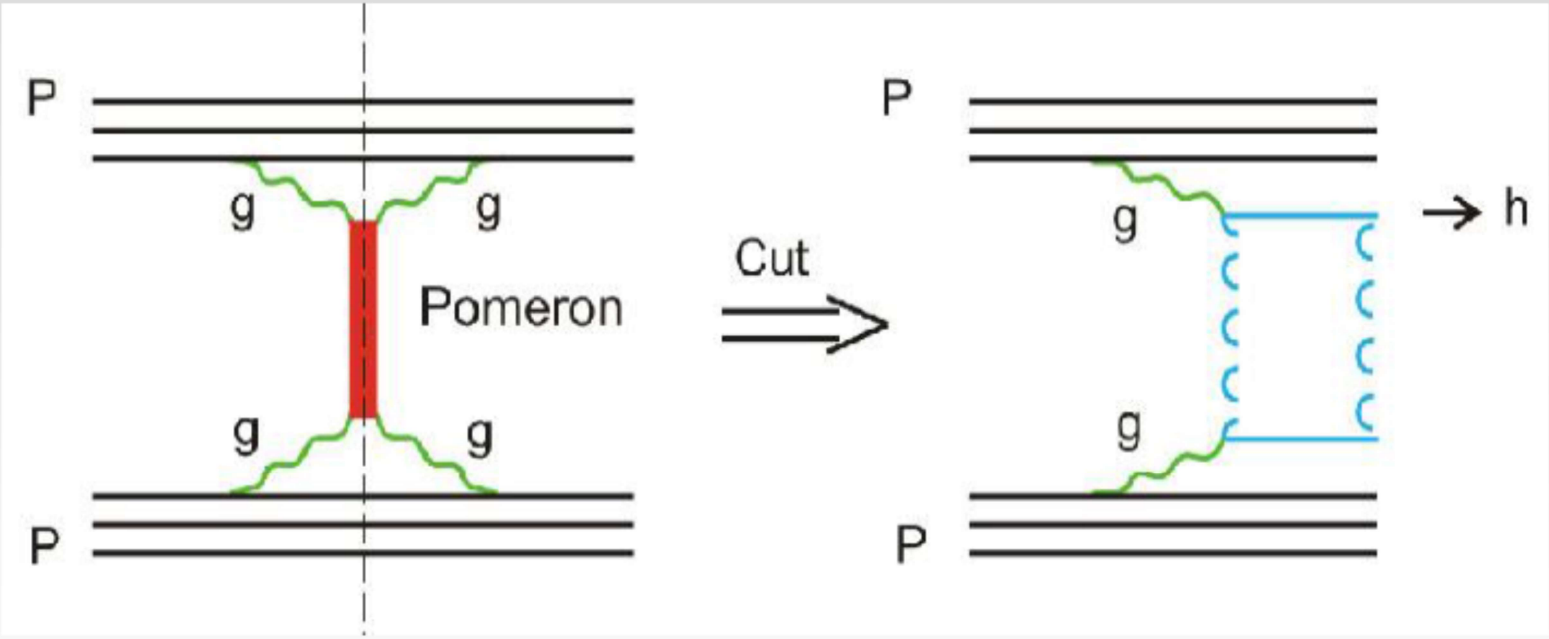

One-Pomeron exchange (left) and the cut one-Pomeron exchange (right); P-proton, g-gluon, h-hadron produced in PP

In the light cone dynamics the proton has a general decomposition:

$|uud\rangle, |uudg\rangle, |uudq\bar{q}\rangle, \ldots$ S.J.Brodsky, C.Peterson, N.Sakai, Phys.Rev. D 23 (1981) 2745.

PP→ charge hadrons +X at $s^{1/2} = 7$ TeV

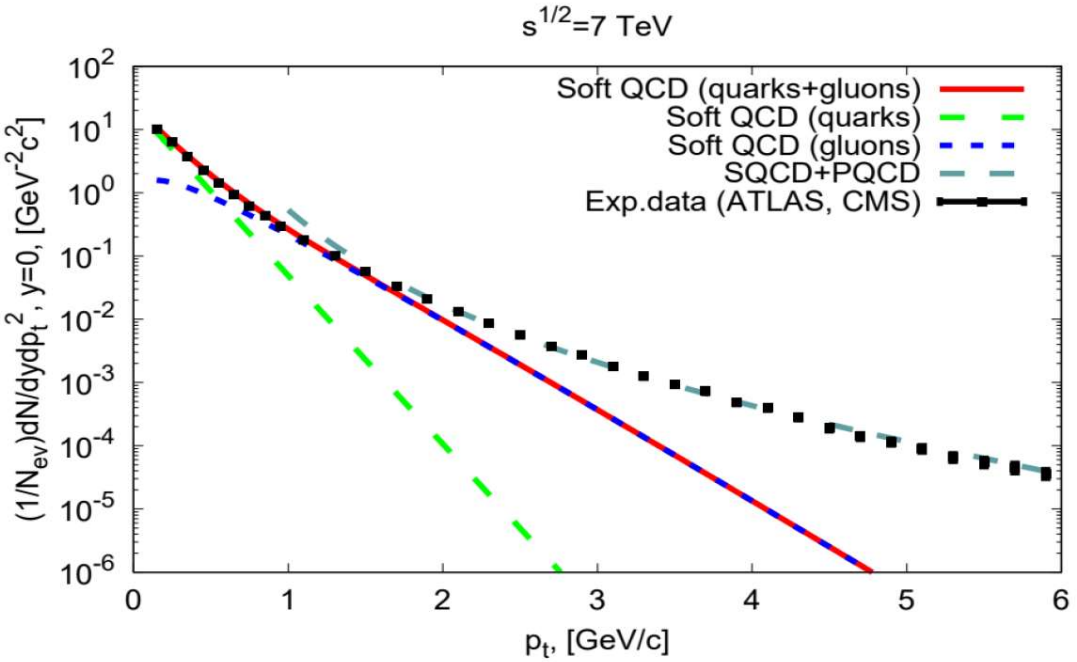

Results of the calculations of the inclusive cross section of charge hadrons produced in pp collisions at the LHC energies as a function of their transverse momentum p_t at √s =7 TeV. The points are the LHC experimental data: ***G. Aad, et al. (ATLAS Collaboration), New J. Phys. 13, 053033 (2011) and V. Khachatryan, et al. (CMS Collaboration), Phys. Rev. Lett. 105, 022002 (2010).***

A.A. Grinyuk, A.V.Lipatov, G.L., N.P.Zotov, *Phys.Rev.* D93, 014035 (2016)

PP → tt + X at $s^{1/2}$ = 13 TeV

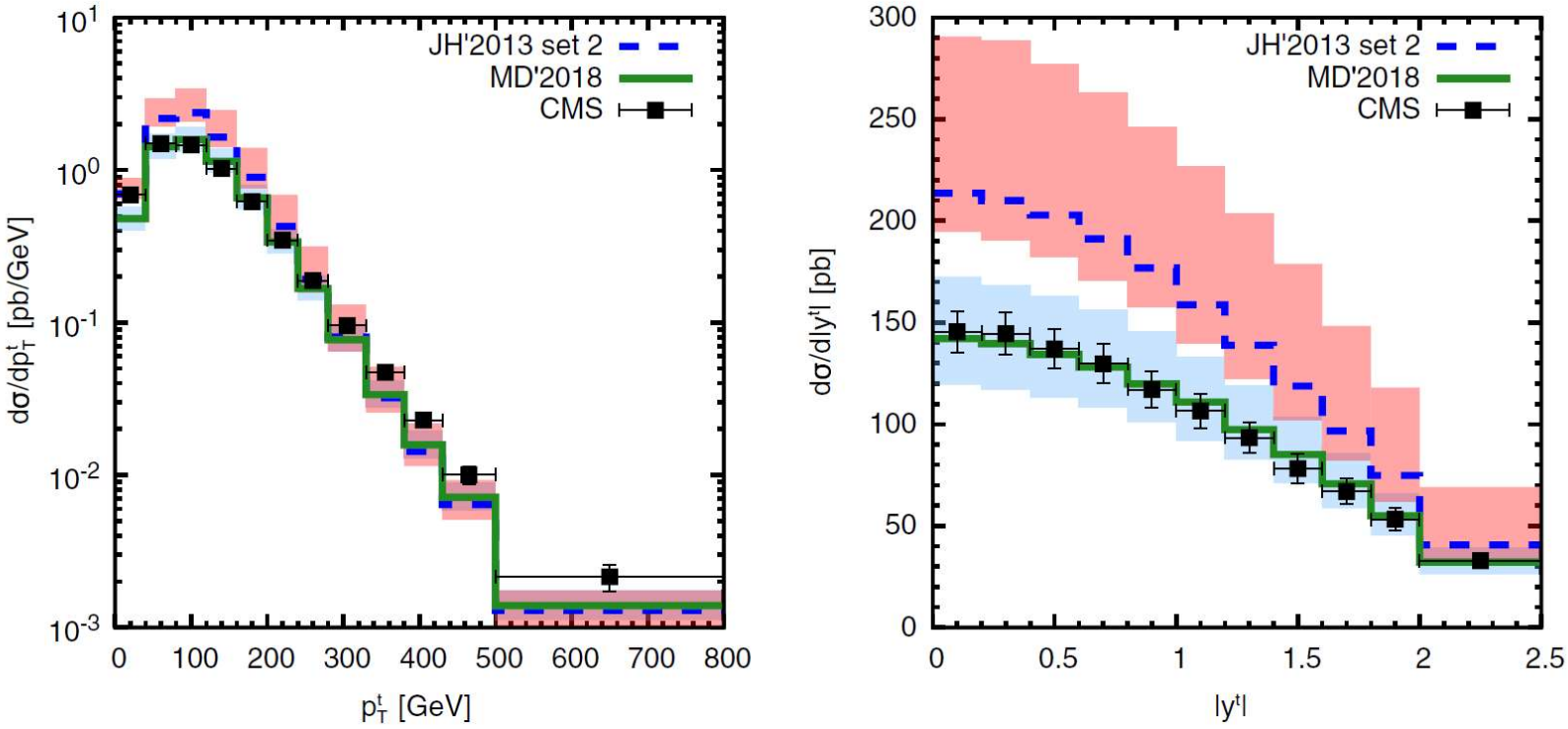

The transverse momentum and rapidity distributions of inclusive *tt* production in *pp* collisions at $s^{1/2}$ = 13 TeV. The green (solid) and blue (dashed) curves correspond to our gluon distribution MD'2018 and set 2 of JH'2013 (DESY). The shaded bands represent the scale uncertainties.

N.A.Abdulov, H.Jung, A.V.Lipatov, G.L., M.A.Malyshev, Phys.Rev., D98, 054010 (2018).

PP → H (→ ZZ*→ 4l) at $s^{1/2}$ = 13 TeV

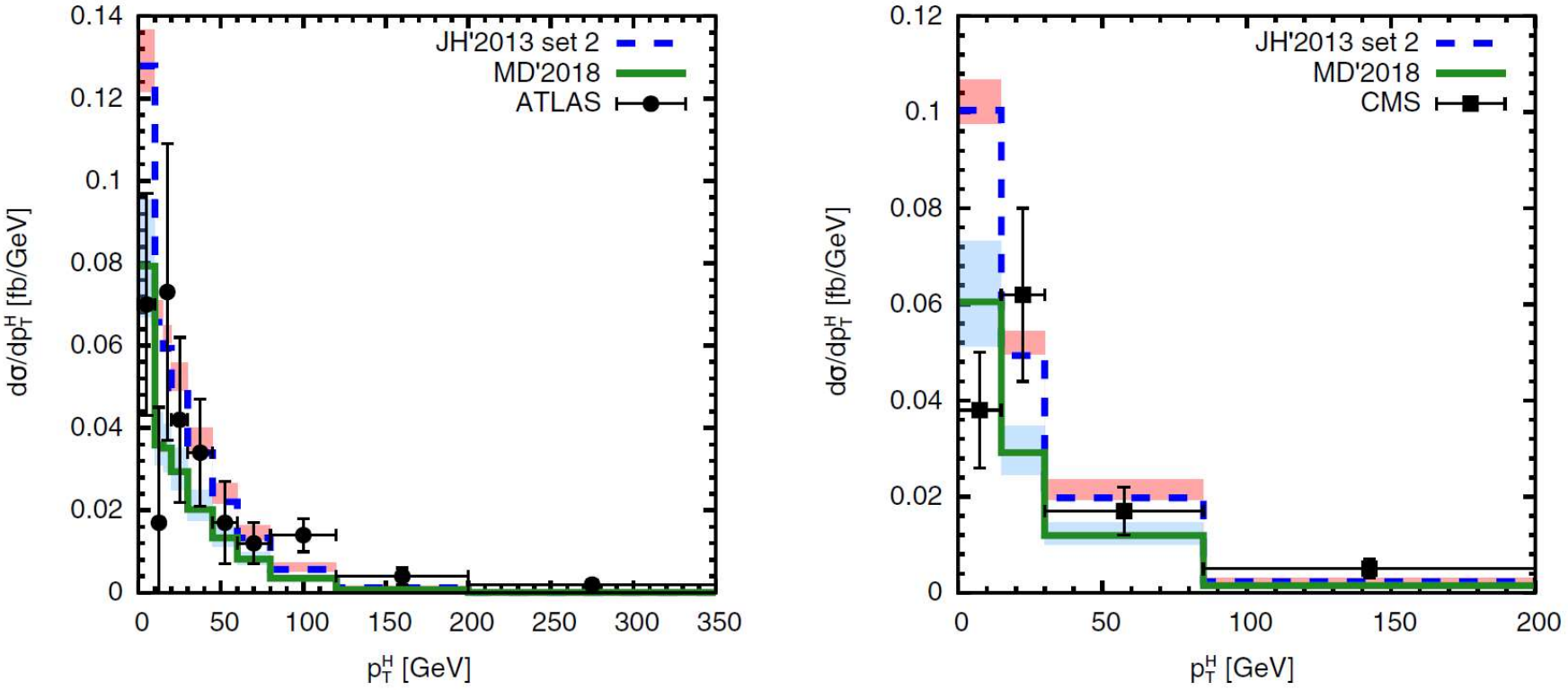

Transverse momentum of Higgsboson decayed into ZZ*→4 leptons.
Left: ATLAS data; right: CMS data

N.A.Abdulov, H.Jung, A.V.Lipatov, G.L., M.A.Malyshev, Phys.Rev., D98, 054010 (2018).

III. Dielectron production and form factor at the time-like region

Direct dielectron production in $\pi^- p \rightarrow e^+ e^- n$

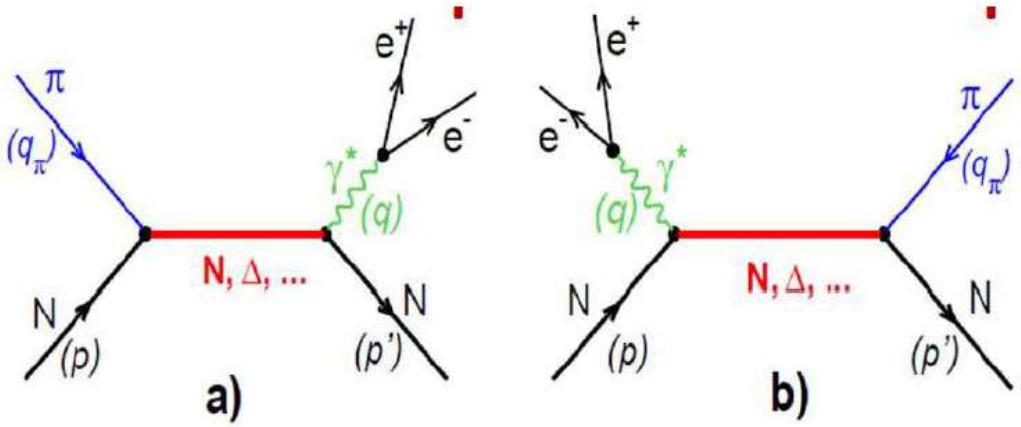

Diagrams, which can give an additional contribution to the direct dielectron production in π-p interaction

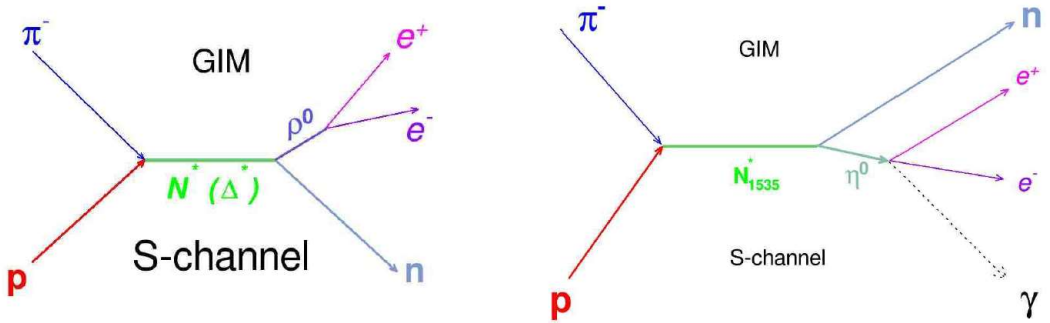

$\pi^- p \to \gamma^* n \to e^+ e^- n$

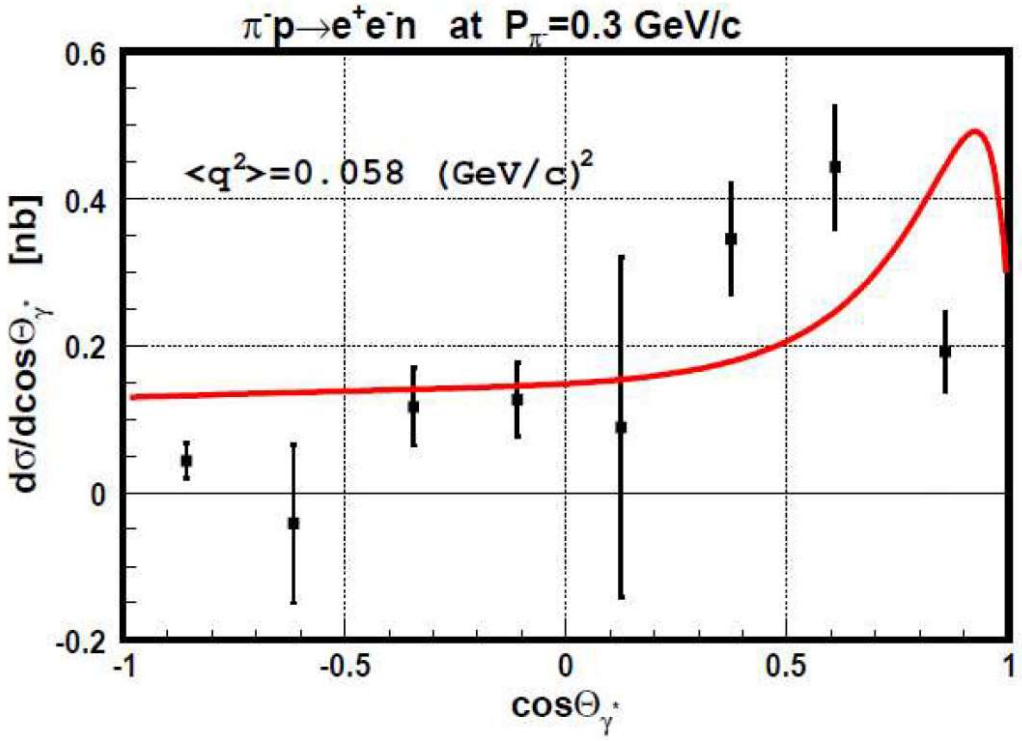

Figure 3: Angular distribution $d\sigma/d\cos\theta_{\gamma^*}$, where θ_{γ^*} is the angle of the virtual photon γ^*. The solid curve corresponds to our calculations. The experimental data are taken from [24].

A.P.Jerusalimov, G.I. Lykasov, arXiv:1704.00311 [hep-ph], PEPAN Lett .v.15, p.457 (2018) .

S. Ph. Berezhnev et al., Sov. J. Nucl. Phys. 24, 591 (1976) -experimental data obtained at JINR, DLNP.

Dielectron production in $\pi^- p \rightarrow e^+ e^- n$

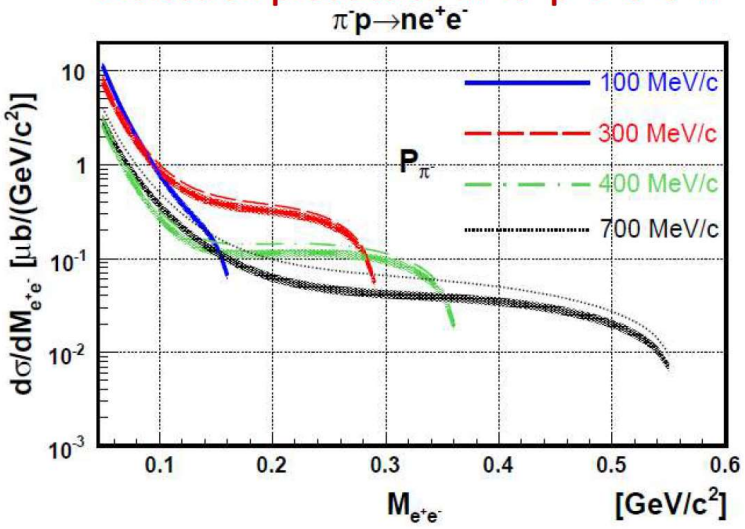

Figure 5: Invariant mass distribution for dielectrons, $d\sigma/dM_{e^+e^-}$, produced in reaction $\pi^- p \to e^+ e^- n$ at different pion momenta. The curves with bands correspond to calculations without any form factors $F(q^2)$ or $F(t)$ including the theoretical uncertainties, while the thin lines dash-dotted, double dash-dotted and dotted correspond initial pion momenta 300MeV/c, 400 MeV/c and 700 MeV/c respectively

Form factor **$F(t) = \Lambda^2 / (\Lambda^2 - t)$, $\Lambda = 1 (GeVc)^{-1}$, at $t>0$ we have $F(t)>1$**

A.P.Jerusalimov, G.I. Lykasov, arXiv:1704.00311 [hep-ph], PEPAN Lett . v.15, p.457 (2018) .

New results

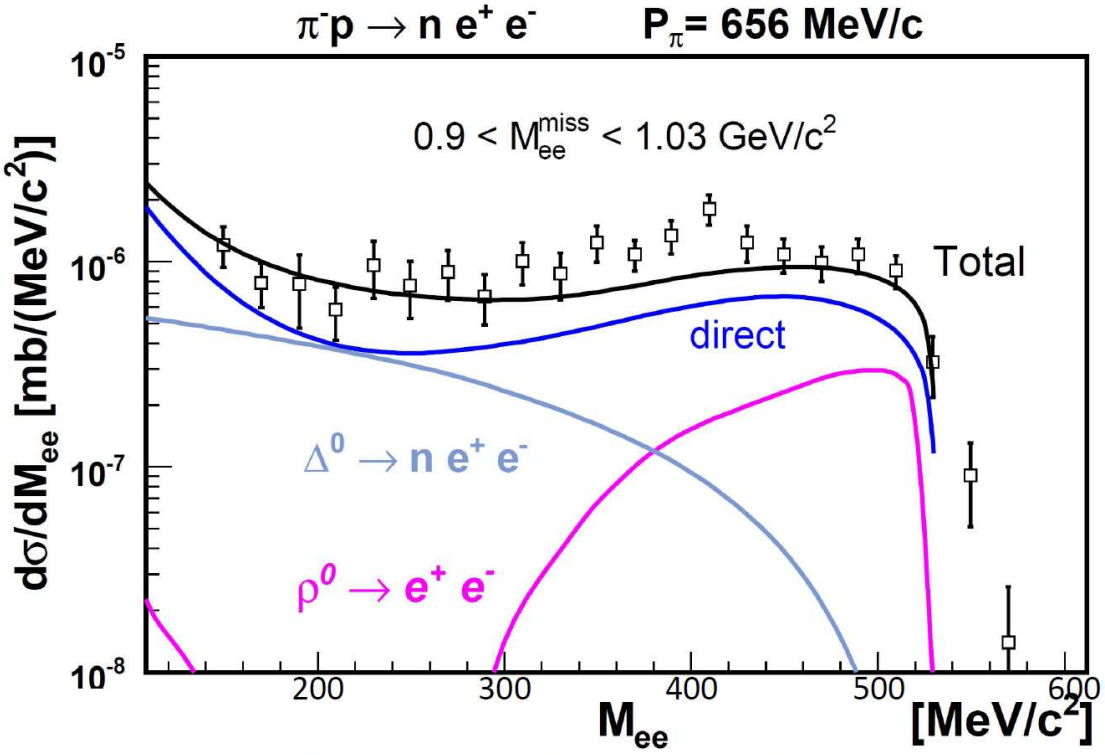

The blue line is our calculation using form factor F = exp(R^2t), where R=3(GeV/c)$^{-1}$, t=(p_π - q)^2 is the transfer, **which can be positive at the time-like region of the virtual photon**.
The black curve is the sum of the direct calculation and channels **π^- p →Δ^0 →n e^+ e^- (Landsberg used by Pluto)** and **π^- p →N^* ρ^0 → n e^+ e^-.**

IV. Some recommendations for the Demin's ecxperiment performed at DLNP

Meso-molecule $pt\mu$ and e^+e^- emission

$$pt \rightarrow {}^4He + 2\gamma$$

$$pt \rightarrow {}^4He + e^+e^-$$

It would be interesting to construct the ratio $I_{2\gamma}/I_{e+e-}$ at different E_0 transitions to look the effect of the time-like form factor.

Number of papers published in reviewed journals for latest 5 years – 17, in proceedings of Conferences – 14.

Citations for 5 years

1. General – 333

2.Maximal citation – 83. Transverse momentum dependent (TMD) parton distributoon functions: status and prospects. (Proc.Conf.) Acta Phys.Polon. B46, 2501 (2015).

3.Intrinsic charm, maximal citation – 49. Searching for intrinsic charm in the proton at the LHC. Phys.Lett. B728, 602 (2014).

4.Inclusive hadron p_T – spectra at mid-rapidity – 56. Systematic properties of the Tsallis distribution: energy dependence of parameters in high-energy p-p collisions. Phys.Lett. B723, 351 (2013).

SUMMARY

1.A first estimate of the intrinsic charm (IC) probability w in the proton has been carried out from the recent ATLAS data.

2.Big experimental and theoretical uncertainties allowed us to estimate only the upper limit of IC w_{ul} = 1.94% at CL=68 %.

3.One needs also the reduce of the theoretical uncertainties related to the QCD scale.

4. The double ratio $\sigma_f(Z+c)/\sigma_c(Z+c))/(\sigma_f(Z+b)/\sigma_c(Z+b))$ is preferable to search for the IC contribution

5. The non perturbartive gluon distribution plays the main role in the QCD Q^2 – evolution equation. Many observables of hard processes are very sensitive to these gluon distributions.

6.The dielectron production, for example, in π-p reactions can give a new information on the πγN form factor at the time like region.

THANK YOU VERY MUCH FOR YOUR ATTENTION !

BACK UP

Single top production in *pp* at $s^{1/2} = 13$ TeV

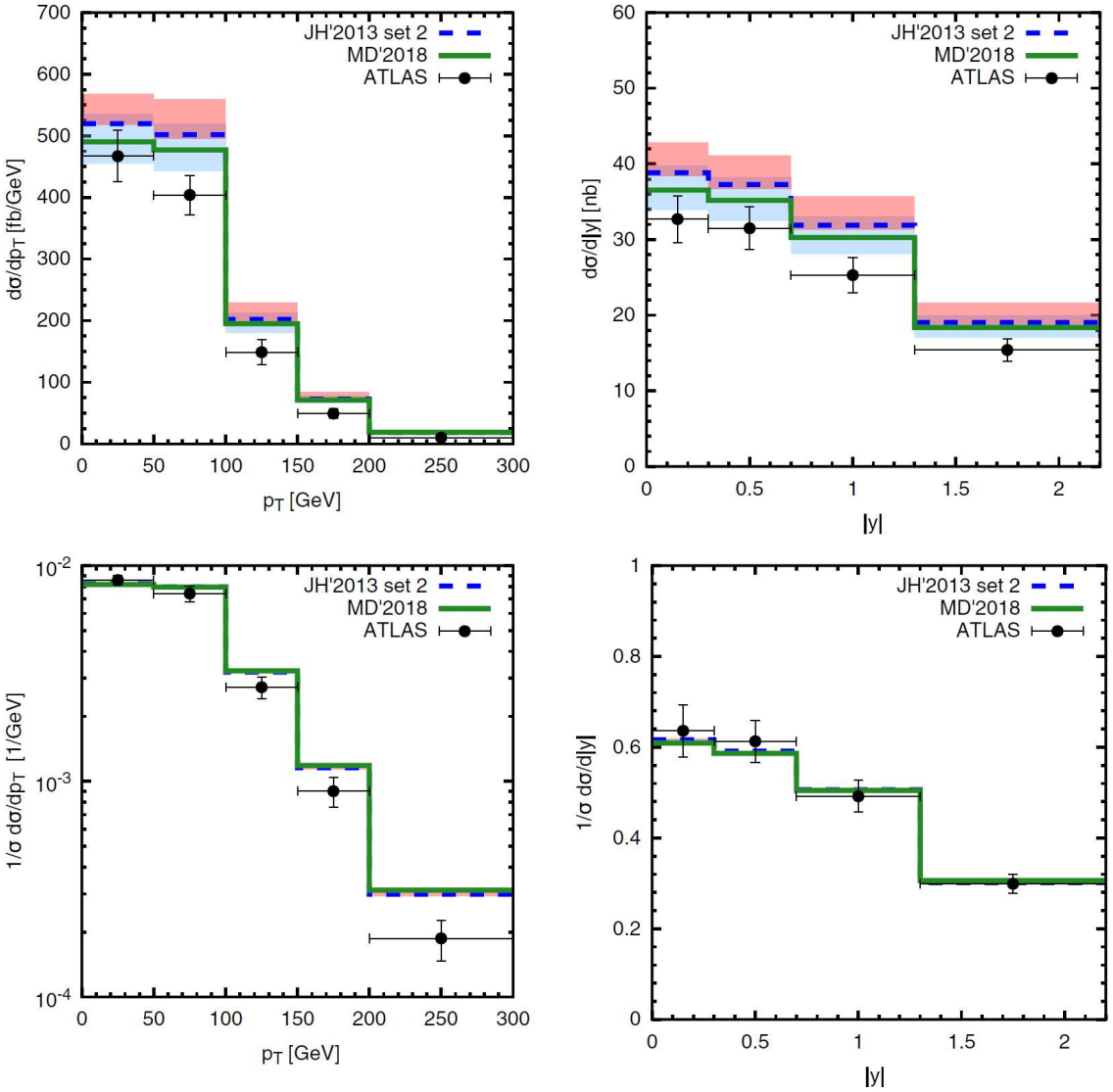

p_T- distribution (left) and y- distribution (right) of top-quark. The points are the ATLAS data.

N.A.Abdulov, H.Jung, A.V.Lipatov, G.L., M.A.Malyshev, Phys.Rev., D98, 054010 (2018).

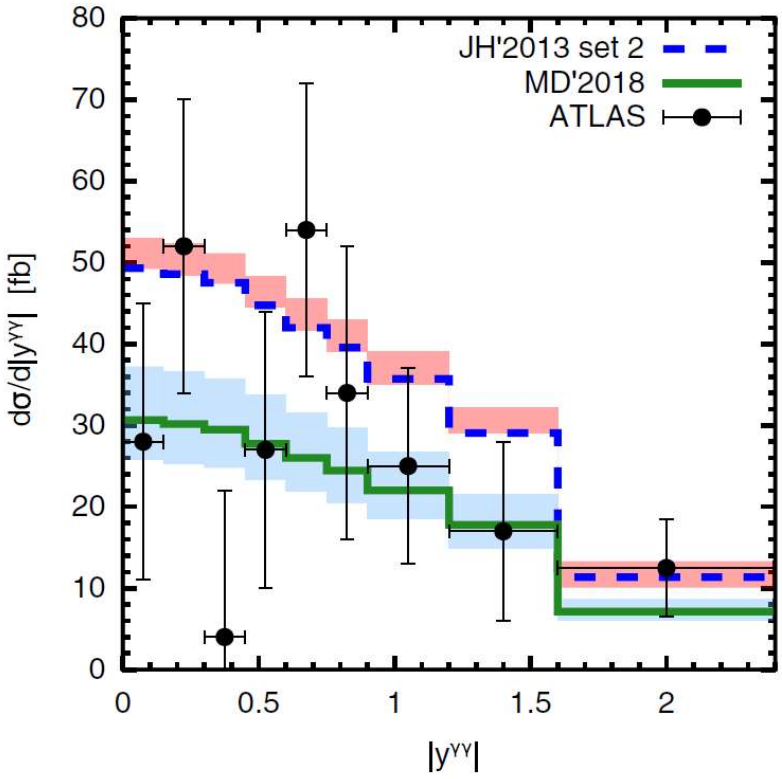
JH'2013 set 2
MD'2018
ATLAS
dσ/d|y^γγ| [fb]
|y^γγ|
0
10
20
30
40
50
60
70
80
0
0.5
1
1.5
2

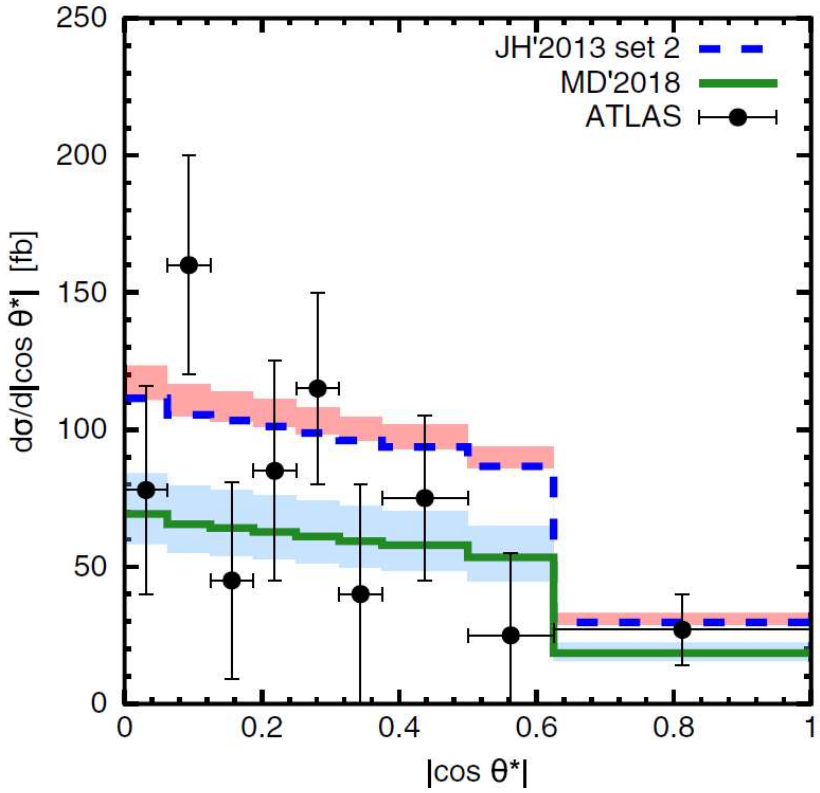
JH'2013 set 2
MD'2018
ATLAS
dσ/d|cos θ*| [fb]
|cos θ*|
0
50
100
150
200
250
0
0.2
0.4
0.6
0.8
1

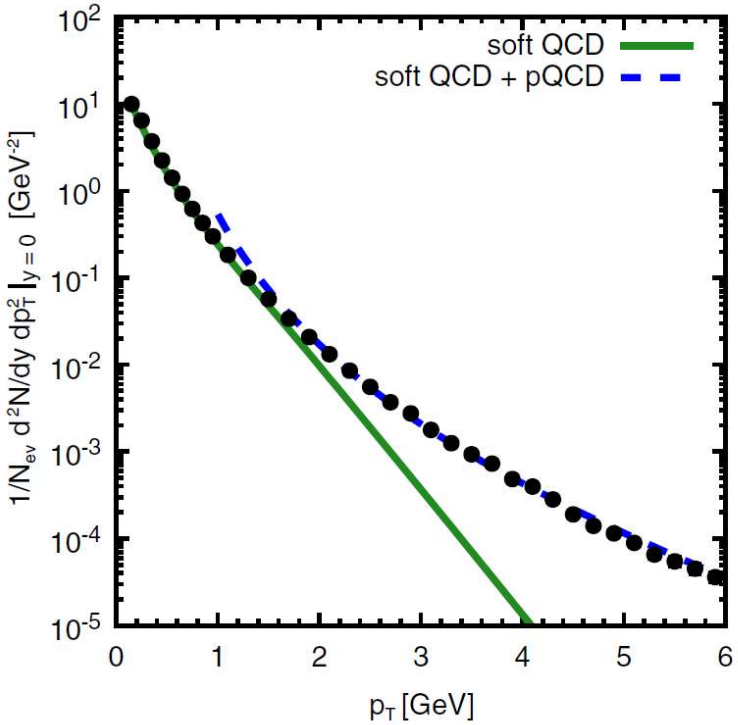
soft QCD
soft QCD + pQCD
$1/N_{ev}\ d^2N/dy\ dp_T^2|_{y=0}$ [GeV^{-2}]
p_T [GeV]

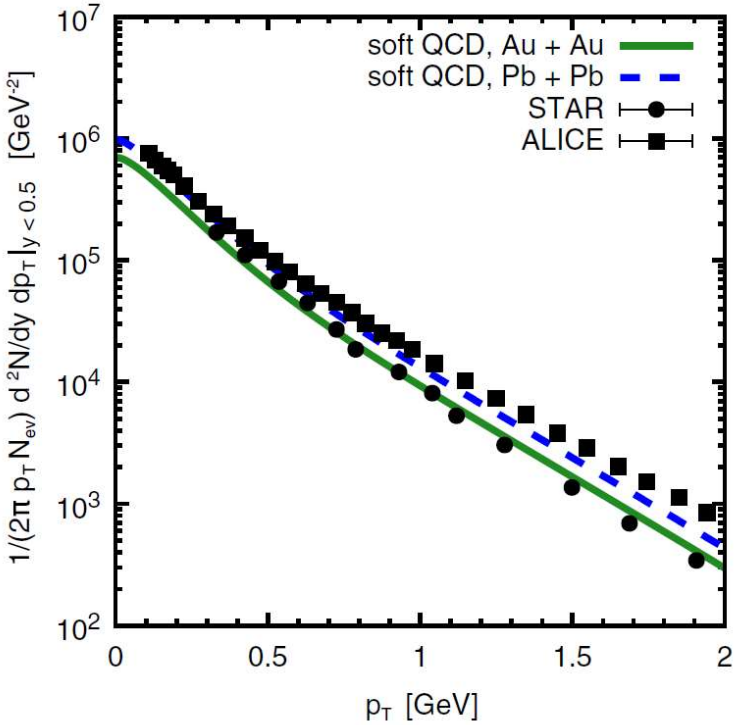
soft QCD, Au + Au
soft QCD, Pb + Pb
STAR
ALICE
$1/(2\pi\ p_T N_{ev})\ d^2N/dy\ dp_T|_{y<0.5}$ [GeV^{-2}]
p_T [GeV]

INTRINSIC HEAVY QUARK STATES

Two types of parton contributions

The extrinsic quarks and gluons are generated on a short time scale in association with a large transverse-momentum reaction.

The intrinsic quarks and gluons exist over a time scale independent of any probe momentum, they are associated with the bound state hadron dynamics.

$$P\left(x_1,\ldots,x_5\right)=N_5\,\delta\left(1-\sum_{i=1}^{5}x_i\right)\left[M_p^2-\sum_{i=1}^{5}\frac{m_i^2}{x_i}\right]^{-2}$$

INTRINSIC HEAVY QUARK DISTRIBUTION

IN PROTON

Integrating $P(x_1,\ldots,x_5)$ over $dx_1 \ldots dx_4$ and neglecting of all quark masses except the charm quark mass we get

$$P(x_5) = \frac{1}{2}\overline{N}_5 x_5^2\left[\frac{1}{3}(1-x_5)(1+10x_5+x_5^2)+2x_5(1+x_5)\ln(1x_5)\right]$$

$$\overline{N}_5 = N_5/\overline{m}_{4,5}^4$$

Where $|uudQ\overline{Q}$ normalization constant . Here $m_4 = m_5 = m_c = m_{\bar{c}}$ is the bar mass of the charmed quark. w_{IQ} determines some probability to find the Fock state $x_5 \to 1$ in the proton.

COMPARISON OF LIGHT AND HEAVY QUARK DISTRIBUTIONS IN PROTON

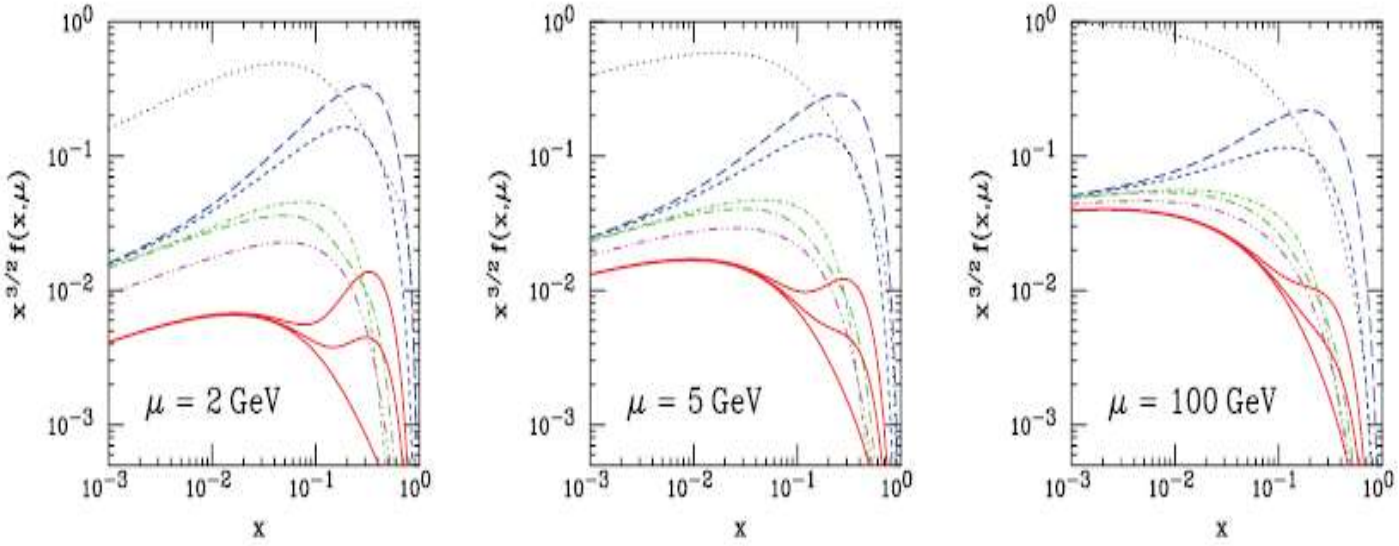

The dotted line is the gluon distribution, the blue long-dashed curve is the valence u-distribution, the blue short-dashed line is the valence d-distribution, the green long-dashed-dotted line is the intrinsic $\bar{u}$, the short dashed-dotted line is the intrinsic $\bar{d}$ distribution , the dashed-dot-dotted is the intrinsic $s=\bar{s}$ and the solid curves are $c=\bar{c}$ with **no IC** (lowest) and with **IC**, $\langle x_{c\bar{c}} \rangle = 0.57\%, 2.\%$ respectively. It is shown that **IC** contribution is larger than $\bar{u}, \bar{d}, \bar{s}$ at x>0.2

PRODUCTION OF HEAVY FLAVOURS IN HARD P-P COLLISIONS

$$E\frac{d\sigma}{d^3p} = \sum_{i,j}\int d^2k_{iT}\int d^2k_{jT}\int_{x_i^{\min}}^{1} dx_i \int_{x_j^{\min}}^{1} dx_j f_i(x_i,k_{iT}) f_j(x_j,k_{jT})\frac{d\sigma_{ij}(\hat{s},\hat{t})}{d\hat{t}}\frac{D_{i,j}^{h}(z_h)}{\pi z_h}$$

$$x_i^{\min} = \frac{x_T\cot(\frac{\theta}{2})}{2 - x_T\tan(\frac{\theta}{2})} \qquad x_F \equiv \frac{2p_z}{\sqrt{s}} = \frac{2p_T}{\sqrt{s}}\frac{1}{\tan\theta} = \frac{2p_T}{\sqrt{s}}\sinh(\eta)$$

$$x_i^{min} = \frac{x_R + x_F}{2 - (x_R - x_F)} \qquad x_R = 2p/\sqrt{s}$$

One can see that $x_i \geq x_F$ If $x_F > 0.1$ then, $x_i > 0.1$ and the conventional sea heavy quark (extrinsic) contributions are suppressed in comparison to the intrinsic ones.

x_F is related to p_T and η . So, at certain values of these variables, in fact, there is no conventional sea heavy quark (extrinsic) contribution. And we can study the IQ contributions in hard processes at the certain kinematical region.

pp →W/Z+heavy flavour jets

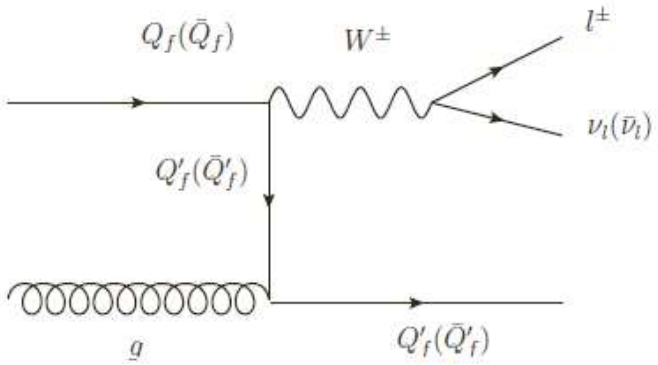

The LO Feynman diagrams for the process $Q_f(\bar{Q}_f)g \to W^{\pm}Q'_f(\bar{Q}'_f)$, where $Q_f = c.b$ and $Q'_f = b, c$ respectively.

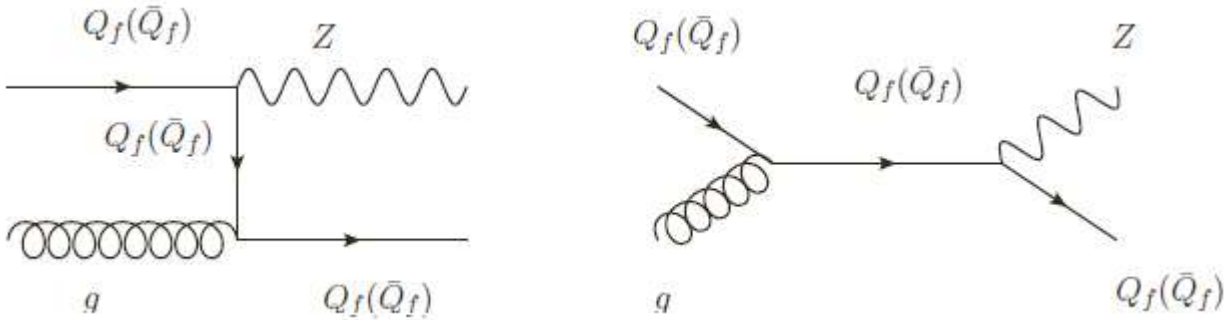

Feynman diagram for the process $Q_f(\bar{Q}_f)g \to ZQ_f(\bar{Q}_f)$

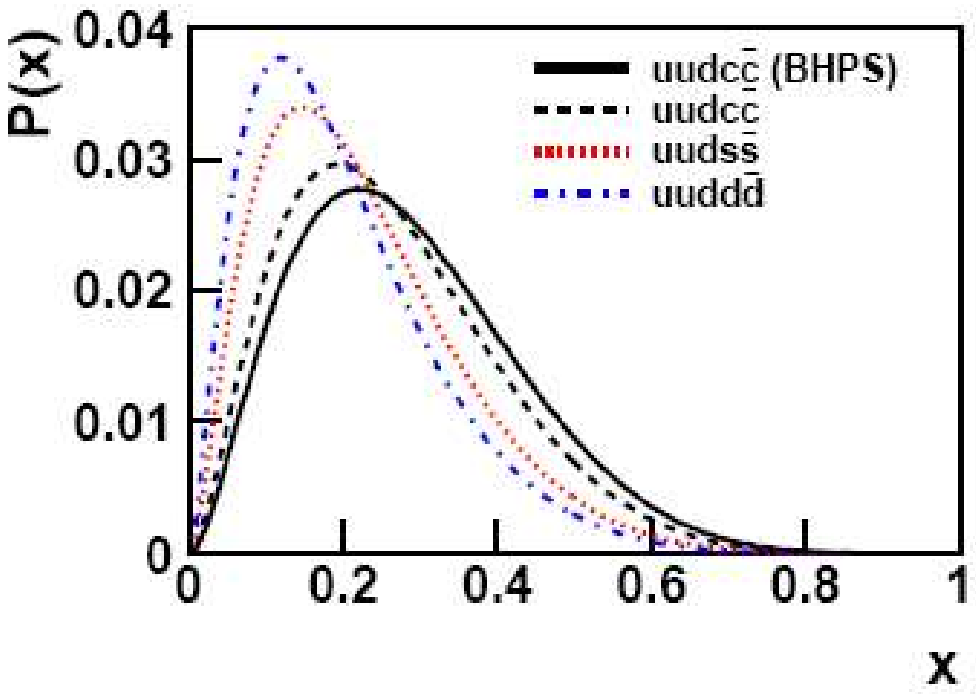

The x-distribution of the intrinsic **Q** calculated within the BHPS model. **There is an enhancement at x > 0.1**

Jen-Chieh Peng & We-Chen Chang, hep-ph/1207.2193.